

## Research Article

# Evaluation on Powder Metallurgy Process Parameters of Ball-Milled AA8079-B<sub>4</sub>C Nanostructured Composites via Taguchi Grey Relational Analysis

M. Meignanamoorthy,<sup>1</sup> Mohanavel Vinayagam,<sup>2</sup> M. Ravichandran,<sup>1,3</sup> T. Raja,<sup>4</sup> Amel Gacem,<sup>5</sup> Amine Mezni,<sup>6</sup> Mohammed Jameel,<sup>7</sup> and Manikandan Ganesan <sup>8</sup>

<sup>1</sup>Department of Mechanical Engineering, K. Ramakrishnan College of Engineering, Trichy 621112, Tamil Nadu, India

<sup>2</sup>Centre for Materials Engineering and Regenerative Medicine, Bharath Institute of Higher Education and Research, Chennai 600073, Tamil Nadu, India

<sup>3</sup>Department of Mechanical Engineering and University Centre for Research & Development, Chandigarh University, Mohali 140413, Punjab, India

<sup>4</sup>Department of Mechanical Engineering, Vel Tech Rangarajan Dr. Sagunthala R&D Institute of Science and Technology, Chennai, 600062 Tamil Nadu, India

<sup>5</sup>Department of Physics, Faculty of Sciences, University 20 Août 1955, Skikda, Algeria

<sup>6</sup>Department of Chemistry, College of Science, Taif University, P.O. Box 11099, Taif 261944, Saudi Arabia

<sup>7</sup>Department of Civil Engineering, College of Engineering, King Khalid University, Abha, Saudi Arabia

<sup>8</sup>Department of Electromechanical Engineering, Faculty of Manufacturing, Institute of Technology, Hawassa University, Ethiopia

Correspondence should be addressed to Manikandan Ganesan; mani301090@hu.edu.et

Received 17 February 2022; Revised 22 April 2022; Accepted 9 June 2022; Published 24 June 2022

Academic Editor: Arpita Roy

Copyright © 2022 M. Meignanamoorthy et al. This is an open access article distributed under the Creative Commons Attribution License, which permits unrestricted use, distribution, and reproduction in any medium, provided the original work is properly cited.

This work made an attempt to optimize the powder metallurgy (PM) process parameters of ball-milled AA8079-B<sub>4</sub>C composites via Taguchi grey relational analysis to attain better mechanical properties. The process parameters are reinforcement weight percentage, compaction pressure, sintering temperature, and sintering time, and the output responses are micro Vickers hardness and compressive strength. The different reinforcement weight percentages are AA8079-x wt.%B<sub>4</sub>C (X = 5, 10, and 15 wt.%). The nanograin-refined green compacts were made at various compaction pressure 200 MPa, 300 MPa, and 400 MPa. The various sintering temperatures are 375°C, 475°C, and 575°C at different sintering times 1 h, 2 h, and 3 h. Taguchi L<sub>27</sub> orthogonal array was utilized to examine the powder metallurgy process parameters. It could be understood from the results that higher reinforcement weight percentage, compaction pressure, and sintering temperature were determined as appropriate parameters to obtain maximum hardness and compressive strength.

## 1. Introduction

Metal matrix composite (MMC) offers a symbiotic blend of properties; this could not be obtained in traditional materials. The MMCs can be attained by combining particulates B<sub>4</sub>C, SiC, Al<sub>2</sub>O<sub>3</sub>, AlN, and Ash into less weight alloys are the preferred to substitute traditional materials in numerous usages defence, structural, automobile, aero-

space, marine, and mining industries [1–3]. Owing to the less density, better specific strength and better thermal conductivity aluminium alloys are extensively utilized [4]. To fulfill the necessities such as better mechanical properties and wear resistance of aluminium matrix composites (AMCs), AMCs are reinforced with outstanding structural, and physical properties are significantly required [5, 6]. Amid the different reinforcements, boron carbide (B<sub>4</sub>C)

possesses extreme hardness subsequent to diamond and cubic boron nitride. Moreover,  $B_4C$  has lesser specific gravity ( $2.51\text{ g/cm}^3$ ), and this is lower than Al ( $2.7\text{ g/cm}^3$ ).  $B_4C$  possesses extreme wear and impact resistance, better resistance to chemical agents, and high melting point [7, 8]. Despite of extreme mechanical properties, the utilization of  $B_4C$  reinforcement has been improved extremely [9, 10].

Powder metallurgy (PM) production method includes various steps, namely, blending of powders, compaction, sintering, and secondary finishing method to manufacture parts with reliable net-shape. Metal components produced through PM can be utilized in automobile, aerospace, defence, and electronic industry because of its superior physical and mechanical properties. Near net shape components can be fabricated via PM method; furthermore, material wastage can be eliminated. Uniform distribution of reinforcement particle with matrix can be attained [11, 12]. Precision metal components can be fabricated through PM route so this technique has been acknowledged as extremely established technique. In the course of the most recent seven eras, the innovation has developed from fabricating bearings for autos to difficult transferor gear set in vehicle transposal and engines connecting rods [13]. Figure 1 shows the process sequence for fabrication of MMC using PM. Nowadays, many of the researchers focused to study the powder metallurgy process parameters such as reinforcement weight percentage, compaction pressure, and sinterability [14–18]. Zakir Hussain et al. [19] examined the powder metallurgy process parameters of diamond–copper composites in terms of compaction pressure, sintering temperature, and holding time and reported that compaction pressure 525 MPa, sintering temperature  $900^\circ\text{C}$ , and holding time 2 h are the most influencing parameters. Pravin et al. [20] utilized Taguchi system to optimize the process parameters of Al-10% Cu composites, and the process parameters are compaction load, lubricant, sintering atmosphere, and dwell time and stated that lubricant is a major influencing parameter. Ravichandran and Anandkrishnan [21] examined the PM parameters to obtain higher strength coefficient in aluminium matrix composite via Taguchi method and described that compaction pressure and sintering temperature are major substantial parameters.

From the detailed literature study, it has been clearly evidenced that many of the researchers investigated the powder metallurgy process parameters as in Figure 1 using different matrix materials and reinforcement particles but none of the work has been carried out in AA8079- $B_4C$  composites. Due to that, an attempt has been taken to optimize powder metallurgy process parameters on the mechanical properties. In general, a material should possess excellent hardness and compressive strength properties then only it can be used for desired application; according to that, this two mechanical properties have been studied by grey Taguchi method.

## 2. Experimental Details

In this investigation, AA8079 powder was produced by mingling the elemental powders Cu, Fe, Si, and Zn with Al pow-

der. Purity of Al, Cu, Fe, Si, and Zn powders is 99.5%, and mesh size as  $10\ \mu\text{m}$  as AA8079 possesses less weight with high strength.  $B_4C$  was selected as reinforcement particle with 99.5% purity and mesh size as  $10\ \mu\text{m}$  as it has excellent hardness; in addition, it has less density, and it is the third hardest reinforcement next to diamond and cubic nitride. The chemical composition of the pure elemental powders is essential to synthesis AA8079 0.05Cu, 1.3Fe, 0.3Si, 0.15Zn, and Al remaining (each one in wt %). The SEM image of the produced AA8079 and as received  $B_4C$  is displayed in Figures 2(a) and 2(b).

Figure 3 shows the details of fabrication of ball milled aluminium alloy and its composites. The needed amount of elemental powders was exactly weighted by utilizing an electronic weight balance machine to produce the composition, AA8079, AA8079-5% $B_4C$ , AA8079-10% $B_4C$ , and AA8079-15% $B_4C$  and ball milled via high energy ball mill for 10 h [22]. The drum speed maintained was 100 rpm [23]. The diameter of the steel ball utilized here was 10 mm, and ball to powder ratio was 10:1 [24].

The ball milled powders were compressed into cylindrical billets (Dia  $24 \times 10\text{ mm}$ ). A computerized universal testing machine capacity of 10 ton has been used to acquire a green compact. Figure 4 shows the compaction press used and other testing process conducted for the present work. The green compacts were compacted at three different compaction pressure 200 MPa, 300 MPa, and 400 MPa. Then, the green compacts were sintered at three different sintering temperatures  $375^\circ\text{C}$ ,  $475^\circ\text{C}$ , and  $575^\circ\text{C}$  at three different sintering times 1 h, 2 h, and 3 h. As per ASTM, E384-08 Vickers hardness test was performed at a load of 0.3 kg and a dwell time of 10 s on the samples [25], and as per ASTM, E9-89a compression strength test was done via computerized universal testing machine [26]. In this investigation, trials were carried out with four parameters, and three level have been selected. Hence, L27 orthogonal array was selected like reinforcement wt. %, compaction pressure, sintering temperature, and sintering time. Table 1 displays the process parameters and their levels, and the details of the experimental plan by means of L27 OA are enumerated in Table 2. Figure 5 shows the procedure followed for Taguchi grey relational analysis in this work.

## 3. Results and Discussions

**3.1. S/N Ratio Analysis.** Taguchi technique is a dominant utensil in value optimization for fabrication routes. Taguchi technique creates use of an unusual design of OA to inspect the worth characteristics over a nominal amount of experiments [27]. Word “signal” indicates the necessary value for the output characteristic, and “noise” indicates the horrible value for the output characteristic. The S/N ratios could be deliberate using Equations (1) and (2)

$$\frac{S}{N} \text{ ratio} = -10 \log (\text{MSD}). \quad (1)$$

MSD is mean square deviation.

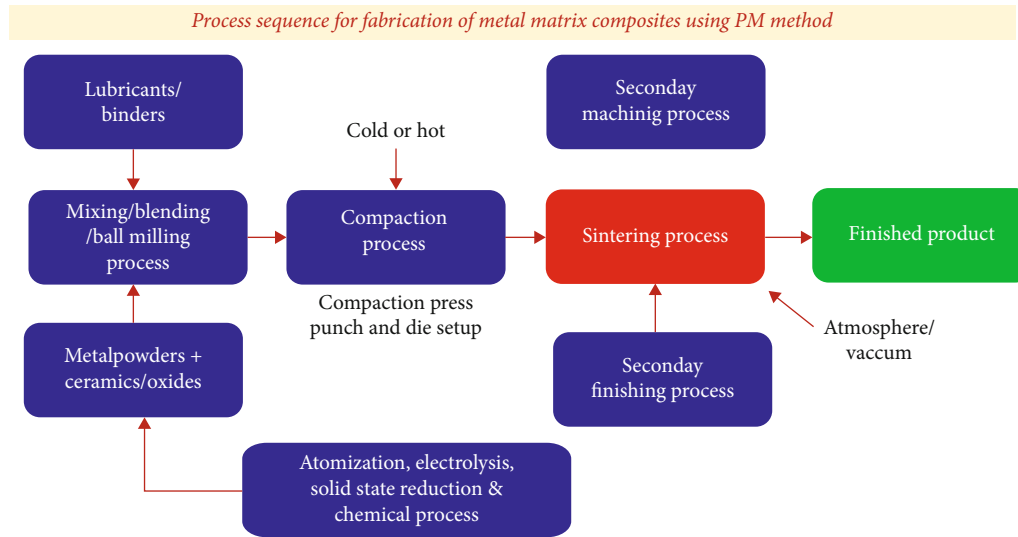


FIGURE 1: Process sequence for fabrication of MMC using PM.

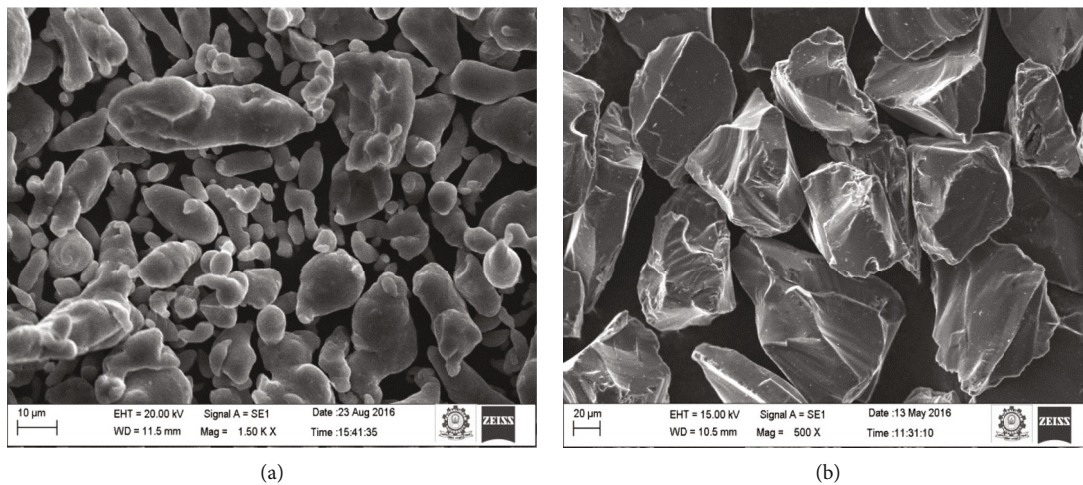


FIGURE 2: (a) SEM images of 10 h ball milled AA8079 powders; (b) as received B<sub>4</sub>C.



FIGURE 3: Fabrication of ball milled aluminium alloy and its composites.

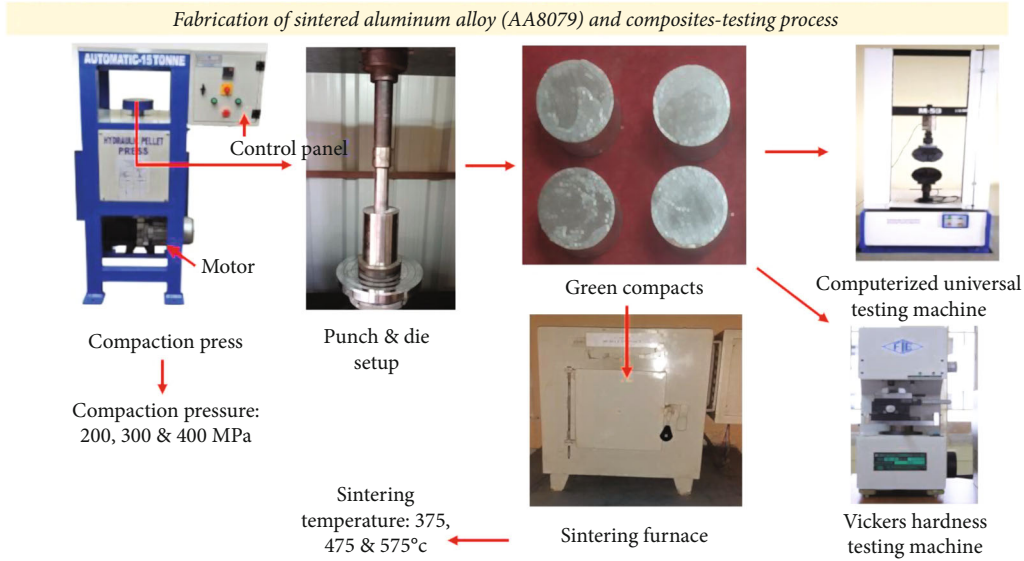


FIGURE 4: Powder metallurgy process to produce alloy and composite samples.

TABLE 1: Process parameters and their levels.

| Symbols | Parameters            | Unit | Level 1 | Level 2 | Level 3 |
|---------|-----------------------|------|---------|---------|---------|
| A       | Reinforcement wt. %   | %    | 5       | 10      | 15      |
| B       | Compaction pressure   | MPa  | 200     | 300     | 400     |
| C       | Sintering temperature | °C   | 375     | 475     | 575     |
| D       | Sintering time        | hr   | 1       | 2       | 3       |

The MSD for the higher the better quality characteristic is expressed as

$$\text{MSD} = \frac{1}{n} \sum_{i=1}^n \frac{1}{T_i^2}. \quad (2)$$

An entire degree of factor was six to four factors. The tests would permanently be carried out extra in numbers than that of designated DOF. Therefore, L27 OA was chosen based as per Taguchi's design of experiments [28].

**3.2. Interaction Effects of Factors.** S/N response table for the microhardness and compressive strength is displayed in Table 3, and S/N response graph is shown in Figure 6, drawn via the results provided in Table 3. The microhardness and compressive strength increase with increasing the reinforcement wt %, compaction pressure, and sintering temperature [29, 30]. Here, the reinforcement wt % has been found to be the supreme active parameter and compaction pressure; sintering temperature and sintering time have been identified to be a slight consequence on mechanical properties founded on S/N ratio. From the Figure 6, it is clearly witnessed that reinforcement wt % is the major noteworthy factor on the response. It is detected that the interaction of reinforcement wt % with compaction pressure is minor at low sintering temperature and noteworthy at higher sintering temperature, the foremost cause is improper bind amid the particles

at low compaction pressure and low sintering temperature; and repeatedly, it decreases the microhardness and compressive strength value of the composites. Interaction of compaction pressure with sintering temperature is minor at low pressure and important at higher pressure. The maximum microhardness and compressive strength are attained when the compaction pressure is higher at sintering temperature [31–35]. The interaction of sintering temperature with sintering time is major at maximum temperature and minor at least temperature for the microhardness, because diffusion of atoms takes place at maximum temperature [36]. They [37] reported that increase in reinforcement wt % and sintering temperature increases the microhardness of the composites. This work [38] reported that rise in compaction pressure and sintering temperature increases the compressive strength.

**3.3. Grey Relational Analysis.** It is one of the easiest and simplest tools to provide exact results. The values of grey relation coefficient, grey relation grade, and its rank of each experiments are arranged in Table 4. The author [39] reported maximum the grey relational grade; the superior would be the multirecital characteristics. Figure 7 displays interaction plot for grey relational grade. Figure 8 displays grey relational response for parameters for instance microhardness and compressive strength. The optimal parameter is acquired from trial 27. Table 5 displays response table of

TABLE 2: Experimental results as per L27 OA.

| Expt. no | Reinforcement (wt%) | Compaction pressure (MPa) | Sintering temperature ( $^{\circ}$ C) | Sintering time (hr) | Compressive strength | Hardness |
|----------|---------------------|---------------------------|---------------------------------------|---------------------|----------------------|----------|
| 1        | 5                   | 200                       | 375                                   | 1                   | 125.49               | 141.59   |
| 2        | 5                   | 200                       | 475                                   | 2                   | 133.74               | 145.27   |
| 3        | 5                   | 200                       | 575                                   | 3                   | 140.05               | 120.09   |
| 4        | 5                   | 300                       | 375                                   | 2                   | 131.48               | 147.92   |
| 5        | 5                   | 300                       | 475                                   | 3                   | 149                  | 149.73   |
| 6        | 5                   | 300                       | 575                                   | 1                   | 142                  | 167.3    |
| 7        | 5                   | 400                       | 375                                   | 3                   | 105.33               | 151.25   |
| 8        | 5                   | 400                       | 475                                   | 1                   | 156.03               | 114.89   |
| 9        | 5                   | 400                       | 575                                   | 2                   | 157.11               | 112.62   |
| 10       | 10                  | 200                       | 375                                   | 1                   | 108.09               | 138.97   |
| 11       | 10                  | 200                       | 475                                   | 2                   | 110.81               | 164.85   |
| 12       | 10                  | 200                       | 575                                   | 3                   | 151.24               | 136.06   |
| 13       | 10                  | 300                       | 375                                   | 2                   | 112.79               | 120.45   |
| 14       | 10                  | 300                       | 475                                   | 3                   | 145.98               | 128.53   |
| 15       | 10                  | 300                       | 575                                   | 1                   | 154.77               | 154.7    |
| 16       | 10                  | 400                       | 375                                   | 3                   | 116.22               | 122.02   |
| 17       | 10                  | 400                       | 475                                   | 1                   | 141.06               | 152.38   |
| 18       | 10                  | 400                       | 575                                   | 2                   | 148                  | 132.41   |
| 19       | 15                  | 200                       | 375                                   | 1                   | 139.09               | 161.56   |
| 20       | 15                  | 200                       | 475                                   | 2                   | 120                  | 126.42   |
| 21       | 15                  | 200                       | 575                                   | 3                   | 122.12               | 165.98   |
| 22       | 15                  | 300                       | 375                                   | 2                   | 147.19               | 145.69   |
| 23       | 15                  | 300                       | 475                                   | 3                   | 150.06               | 184.41   |
| 24       | 15                  | 300                       | 575                                   | 1                   | 156.88               | 159.14   |
| 25       | 15                  | 400                       | 375                                   | 3                   | 145.02               | 151.77   |
| 26       | 15                  | 400                       | 475                                   | 1                   | 164.33               | 174.2    |
| 27       | 15                  | 400                       | 575                                   | 2                   | 171                  | 158.03   |

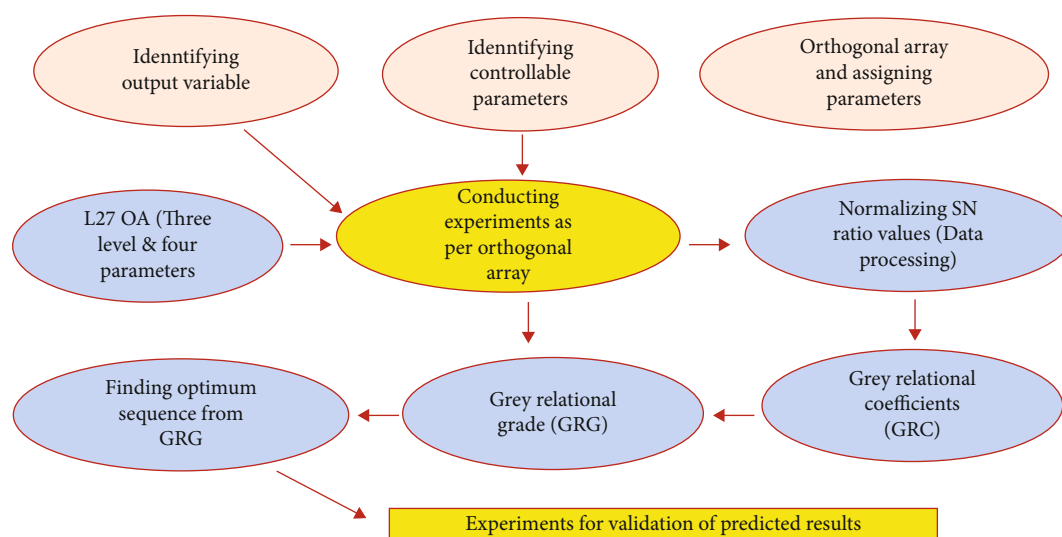


FIGURE 5: Procedure for Taguchi grey relational analysis.



TABLE 3: Response table normalized SN ratios.

| Expt. no | Normalized S/N ratios |                      |
|----------|-----------------------|----------------------|
|          | Microhardness         | Compressive strength |
| 1        | 0.403538              | 0.306989             |
| 2        | 0.454799              | 0.432618             |
| 3        | 0.104053              | 0.528704             |
| 4        | 0.491712              | 0.398203             |
| 5        | 0.516924              | 0.664992             |
| 6        | 0.761666              | 0.558398             |
| 7        | 0.538097              | 0                    |
| 8        | 0.03162               | 0.772042             |
| 9        | 0                     | 0.788488             |
| 10       | 0.367043              | 0.042028             |
| 11       | 0.727539              | 0.083448             |
| 12       | 0.326508              | 0.699102             |
| 13       | 0.109068              | 0.113598             |
| 14       | 0.221619              | 0.619004             |
| 15       | 0.586154              | 0.752855             |
| 16       | 0.130937              | 0.165829             |
| 17       | 0.553838              | 0.544084             |
| 18       | 0.275665              | 0.649764             |
| 19       | 0.681711              | 0.514086             |
| 20       | 0.192227              | 0.22339              |
| 21       | 0.743279              | 0.255672             |
| 22       | 0.460649              | 0.63743              |
| 23       | 1                     | 0.681133             |
| 24       | 0.648001              | 0.784986             |
| 25       | 0.545341              | 0.604386             |
| 26       | 0.85778               | 0.898432             |
| 27       | 0.632539              | 1                    |

the average grey relational grade for every level of the parameters. According to these stages, average grey relational grade has been identified; (i) grey relational grades have been combined via factor equal for every column in the orthogonal array and (ii) average obtained [40]. The abovementioned step has been repeated to determine the normal grey relational grade values for every level of the parameters. They [41] reported that average grey relational grade indicates the level of correlation amid reference sequence and the comparability sequence, the superior the value of the grey relational grade, the stronger the correlation to the reference sequence.

The optimal process parameter combination is achieved from Table 5. The optimal reinforcement weight percent level 3; optimal compaction pressure level 2; optimal sintering temperature, level 3 and duration, level 1; and the best combination of process parameters,  $A_3 B_2 C_3 D_1$ . The optimal process parameters values are reinforcement content 15 wt %, compaction pressure 400 MPa, sintering temperature 575°C, and sintering time 1 h. It could be understood from the Table 6 the maximum value is 0.1479, and the equivalent control factor, i.e., the reinforcement wt % has

the strongest effect on multiperformance characteristics. The order of consequence of the process parameter is factor A (reinforcement wt %), B (sintering temperature), C (compaction pressure), and D (sintering time), i.e.,  $0.1479 > 0.1179 > 0.0907 > 0.0620$ . Factor A is utmost important influence in the process for the multiperformance characteristics.

**3.4. ANOVA.** From ANOVA in Table 7, it is detected that the reinforcement weight %, sintering temperature, and compaction pressure are vital parameters from the  $F$  values. The sintering temperature is the most second influential parameter. The compaction pressure has been considered as third dominant part on the responses. Reinforcement weight % is notable as utmost serious factor with highest contribution percentage as shown in Figure 9. The compaction pressure, sintering temperature, and sintering time are subsidized fair with contributions. Figure 9 shows the contribution plot for all the parameters drawn from ANOVA table.

Sintering normal for  $Al_2O_3$ -reinforced 2xxx series Al composite powders was explored to acquire improved densification. The dissemination of the fluid stage was speedier in the composite powder sintered example than in the mixed powder sintered example. The outcomes demonstrate that a more prominent measure of fluid stage is expected to improve the sinterability of 2xxx series Al composite materials [42]. From Tables 3–6, the ideal parameters for the compressive strength and hardness can be anticipated as the reinforcement weight 15%, compaction pressure 400 MPa, the sintering temperature 575°C, and the sintering time 1 h. This result is near the S/N and ANOVA comes about.

**3.5. Confirmation Test.** Five examples were finished with  $A_3B_2C_3D_1$  parameters, and their normal quality coefficient was found. Table 8 reveals the relationship of the predicted quality coefficient and real quality coefficient of this composite preforms. A low rate blunder of 2.2% is gotten amid anticipated; what is more, trial esteem is demonstrating a decent relationship as appeared in Table 8.

**3.6. Microstructure Analysis of the Composites Produced by Anticipated Parameters.** SEM analysis had been conducted for the samples fabricated from the predicted parameters ( $A_3B_2C_3D_1$ ), and the images are shown in Figures 10(a) and 10(b). From the SEM images, the occurrence of weight percentage of  $B_4C$  particles in the AA8079 matrix was attained. The foremost factors manipulating the microstructure of PM components are compaction pressure along with sintering temperature as per the results obtained from the present study. It is observed from Figures 10(a) and 10(b) that the higher compaction pressure and sintering temperature enhance proper bonding amid  $B_4C$  particles and AA8079 matrix. This creates denser structure owing to greater diffusion rates results in fine microstructure. The uniform distribution of  $B_4C$  particles in Figure 10(b) is evident in the proper identification PM parameters from the TGRA. This proper microstructure of the composite sample enhanced the properties such as CS and hardness.

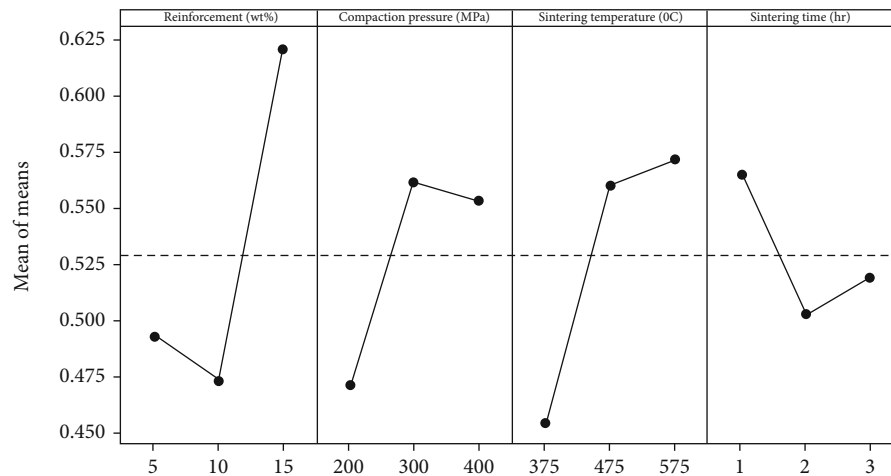


FIGURE 6: S/N ratio response graph for microhardness and compressive strength.

TABLE 4: Grey relational coefficient.

| Expt. no. | Grey relation coefficient |                      | Grey relational grade | Rank |
|-----------|---------------------------|----------------------|-----------------------|------|
|           | Microhardness             | Compressive strength |                       |      |
| 1         | 0.456012                  | 0.419108             | 0.43756               | 22   |
| 2         | 0.478377                  | 0.468436             | 0.473406              | 19   |
| 3         | 0.35818                   | 0.514776             | 0.436478              | 21   |
| 4         | 0.49589                   | 0.453804             | 0.474847              | 18   |
| 5         | 0.508608                  | 0.598796             | 0.553702              | 8    |
| 6         | 0.6772                    | 0.53101              | 0.604105              | 6    |
| 7         | 0.519803                  | 0.333333             | 0.426568              | 23   |
| 8         | 0.340511                  | 0.686853             | 0.513682              | 15   |
| 9         | 0.333333                  | 0.702729             | 0.518031              | 14   |
| 10        | 0.441323                  | 0.342942             | 0.392133              | 24   |
| 11        | 0.647282                  | 0.35297              | 0.500126              | 16   |
| 12        | 0.426079                  | 0.624299             | 0.525189              | 13   |
| 13        | 0.359471                  | 0.360646             | 0.360059              | 27   |
| 14        | 0.39112                   | 0.56754              | 0.47933               | 17   |
| 15        | 0.547138                  | 0.669214             | 0.608176              | 5    |
| 16        | 0.365213                  | 0.374765             | 0.369989              | 26   |
| 17        | 0.52845                   | 0.523059             | 0.525755              | 12   |
| 18        | 0.408385                  | 0.588072             | 0.498229              | 16   |
| 19        | 0.611031                  | 0.507143             | 0.559087              | 7    |
| 20        | 0.382329                  | 0.391662             | 0.386996              | 25   |
| 21        | 0.660746                  | 0.401823             | 0.531284              | 10   |
| 22        | 0.481069                  | 0.579663             | 0.530366              | 11   |
| 23        | 1                         | 0.6106               | 0.8053                | 1    |
| 24        | 0.586855                  | 0.699287             | 0.643071              | 4    |
| 25        | 0.523747                  | 0.558276             | 0.541011              | 9    |
| 26        | 0.778549                  | 0.831161             | 0.804855              | 2    |
| 27        | 0.576395                  | 1                    | 0.788198              | 3    |

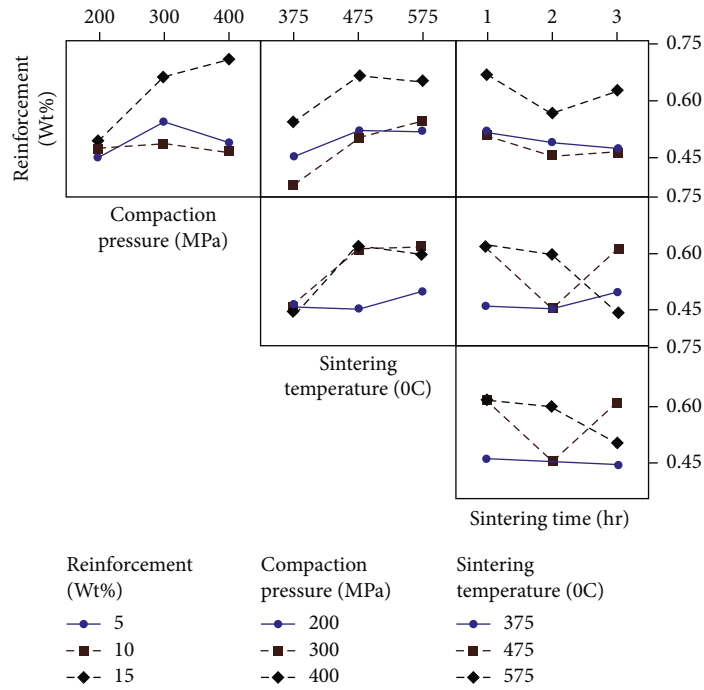


FIGURE 7: Interaction plot for grey relational grade.

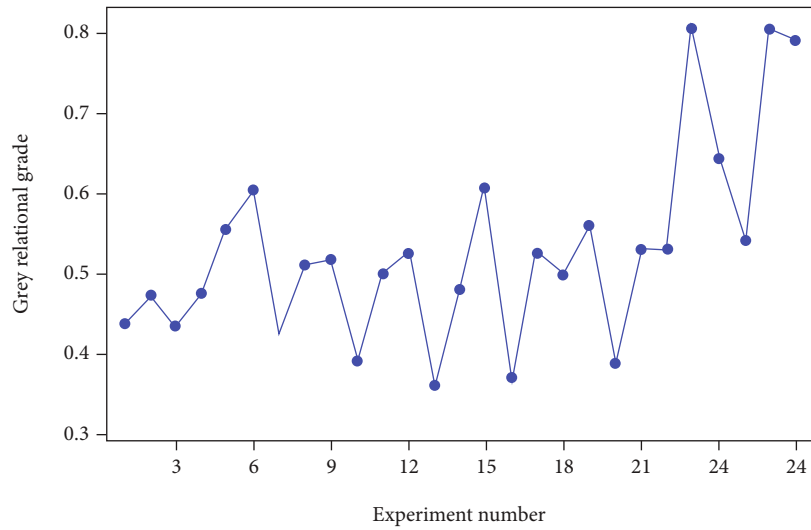


FIGURE 8: GRGs for response parameters (MH, CS).

TABLE 5: Grey relational grade for each level of parameters.

| Factor | Parameters            | Level 1 | Level 2 | Level 3 | Delta | Rank |
|--------|-----------------------|---------|---------|---------|-------|------|
| A      | Reinforcement wt. %   | -6.195  | -6.622  | -4.367  | 2.255 | 1    |
| B      | Compaction pressure   | -6.601  | -5.198  | -5.384  | 1.403 | 3    |
| C      | Sintering temperature | -6.954  | -5.269  | -4.961  | 1.992 | 2    |
| D      | Sintering time        | -5.128  | -6.160  | -5.896  | 1.032 | 4    |



TABLE 6: Response table for means.

| Factor | Parameters            | Level 1 | Level 2 | Level 3 | Delta  | Rank |
|--------|-----------------------|---------|---------|---------|--------|------|
| A      | Reinforcement wt. %   | 0.4932  | 0.4732  | 0.6211  | 0.1479 | 1    |
| B      | Compaction pressure   | 0.4714  | 0.5621  | 0.5540  | 0.0907 | 3    |
| C      | Sintering temperature | 0.4546  | 0.5604  | 0.5725  | 0.1179 | 2    |
| D      | Sintering time        | 0.5654  | 0.5034  | 0.5188  | 0.0620 | 4    |

TABLE 7: Analysis of variance for grey relational grade, using adjusted SS for tests.

| Source                | DF | Adj SS   | Adj MS   | F value | P value |
|-----------------------|----|----------|----------|---------|---------|
| Reinforcement wt. %   | 2  | 0.115957 | 0.057979 | 8.61    | 0.002   |
| Compaction pressure   | 2  | 0.045403 | 0.022702 | 3.37    | 0.057   |
| Sintering temperature | 2  | 0.075683 | 0.037842 | 5.62    | 0.013   |
| Sintering time        | 2  | 0.018770 | 0.009385 | 1.39    | 0.274   |
| Error                 | 18 | 0.121183 | 0.006732 |         |         |
| Total                 | 26 |          |          |         |         |

S = 0.0820511; R - Sq = 67.86%; R - Sq(adj) = 53.57%.

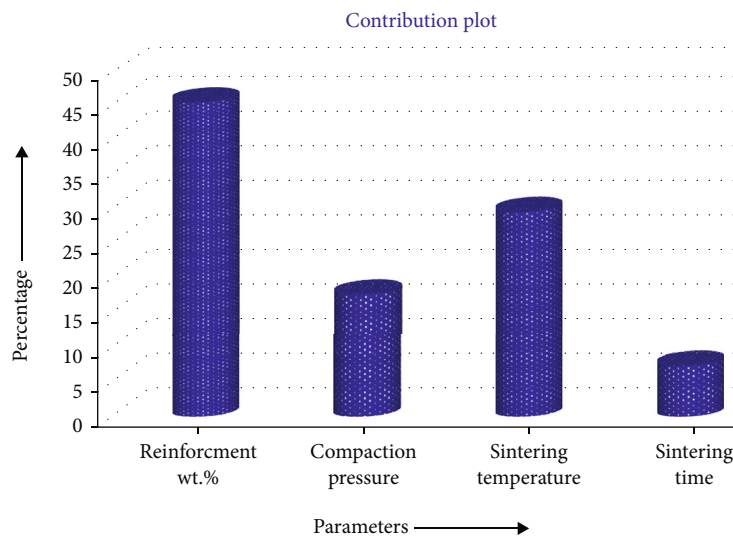


FIGURE 9: Contribution plot from ANOVA.

TABLE 8: Confirmation results.

| Parameter            | Optimal process parameters |            |
|----------------------|----------------------------|------------|
|                      | Predicted                  | Experiment |
| Microhardness        | $A_3B_2C_3D_1$             | 190 VHN    |
| Compressive strength |                            | 177 MPa    |

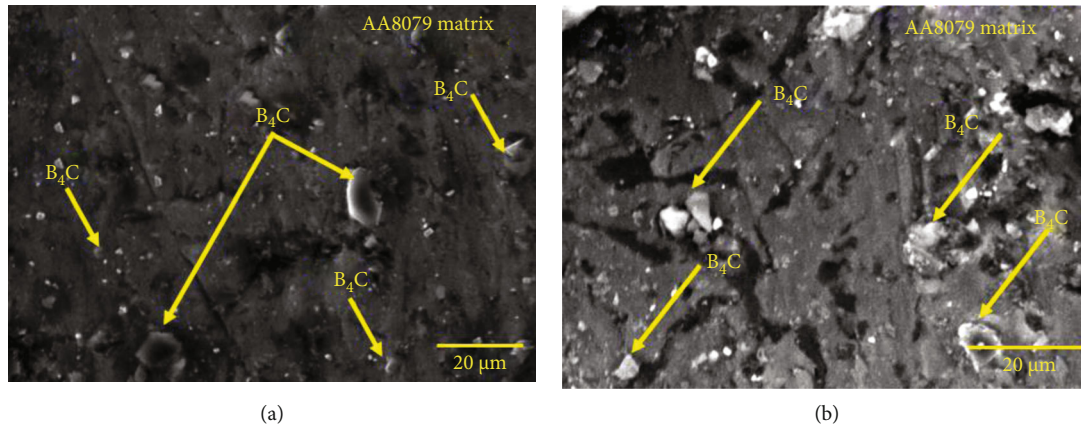


FIGURE 10: (a, b) SEM image of the AA8079-15%B<sub>4</sub>C composites fabricated as per the optimized PM parameters.

#### 4. Conclusions

The subsequent conclusions have been strained from the investigations conducted on the AA8079-B<sub>4</sub>C composites under various process parameters.

The AA8079-B<sub>4</sub>C composites were fabricated via powder metallurgy manufacturing method.

The influence of powder metallurgy process parameters on AA8079-B<sub>4</sub>C composites was studied.

The important parameters reinforcement weight percentage, compaction pressure, sintering temperature, and sintering time were analysed by using Taguchi grey analysis on the responses such as hardness and compressive strength of AA8079-B<sub>4</sub>C samples.

Amid the parameters, reinforcement weight percentage 15%, sintering temperature 575°C, compaction pressure 400 MPa, and sintering time 1 h shows a positive consequence on the mechanical properties.

SEM examination on the AA8079-B<sub>4</sub>C sintered composites fabricated by the optimized parameters shows the homogenous dispersal of the reinforcement with the matrix and good bonding between the matrix and reinforcement.

In future, the same results were optimized by using some other optimization tools like genetic algorithm and neural network.

#### Data Availability

The data used to support the findings of this study are included within the article. Further data or information is available from the corresponding author upon request.

#### Conflicts of Interest

The authors declare that there are no conflicts of interest regarding the publication of this paper.

#### Acknowledgments

The authors appreciate the supports from Hawassa University, Ethiopia, for the research and preparation of the manuscript. This study was funded by Taif University Researchers Sup-

porting Project number (TURSP-2020/28), Taif University, Taif, Saudi Arabia.

#### References

- [1] V. Mohanavel, K. Rajan, and M. Ravichandran, "Synthesis, characterization and properties of stir cast AA6351-aluminium nitride (AlN) composites," *Journal of Materials Research*, vol. 31, no. 24, pp. 3824–3831, 2016.
- [2] M. L. Bharathi, S. Adarsh Rag, L. Chitra et al., "Investigation on wear characteristics of AZ91D/nanoalumina composites," *Journal of Nanomaterials*, vol. 2022, Article ID 2158516, 9 pages, 2022.
- [3] M. Meignanamoorthy and M. Ravichandran, "Synthesis, properties and microstructure of sintered and hot extruded boron carbide reinforced AA8079 (Al-Cu-Fe-Si-Zn) matrix composites," *Materials Research Express*, vol. 5, no. 11, p. 116508, 2018.
- [4] R. Guan, Y. Wang, S. Zheng et al., "Fabrication of aluminum matrix composites reinforced with Ni-coated graphene nanosheets," *Materials Science and Engineering A*, vol. 754, pp. 437–446, 2019.
- [5] B. Chen, J. Shen, X. Ye et al., "Length effect of carbon nanotubes on the strengthening mechanisms in metal matrix composites," *Acta Materialia*, vol. 140, pp. 317–325, 2017.
- [6] M. Ravichandran, V. Mohanavel, T. Sathish, P. Ganeshan, S. S. Kumar, and R. Subbiah, "Mechanical properties of AlN and molybdenum disulfide reinforced aluminium alloy matrix composites," *Journal of Physics: Conference Series*, vol. 2027, p. 012010, 2021.
- [7] A. Alizadeh and M. J. Abdollahi Aand Radfar, "Processing, characterization, room temperature mechanical properties and fracture behavior of hot extruded multi-scale B<sub>4</sub>C reinforced 5083 aluminum alloy based composites," *Transactions of Nonferrous Metals Society of China*, vol. 27, no. 6, pp. 1233–1247, 2017.
- [8] A. Sivkov, I. Rakhmatullin, I. Shanenkov, and Y. Shanenkova, "Boron carbide B<sub>4</sub>C ceramics with enhanced physico-mechanical properties sintered from multimodal powder of plasma dynamic synthesis," *International Journal of Refractory Metals and Hard Materials*, vol. 78, pp. 85–91, 2019.
- [9] Y. H. Celik and K. Secilmis, "Investigation of wear behaviours of Al matrix composites reinforced with different B<sub>4</sub>C rate

- produced by powder metallurgy method,” *Advanced Powder Technology*, vol. 28, no. 9, pp. 1–7, 2017.
- [10] J. A. Jeffrey, S. S. Kumar, V. A. Roseline, A. L. Mary, and D. Santhosh, “Contriving and assessment of magnesium alloy composites augmented with boron carbide VIA liquid metallurgy route,” *Materials Science Forum*, vol. 1048, pp. 3–8, 2022.
- [11] A. Gokce, F. Findik, and A. O. Kurt, “Microstructural examination and properties of premixed Al-Cu-Mg powder metallurgy alloy,” *Materials Characterization*, vol. 62, no. 7, pp. 730–735, 2011.
- [12] M. Meignanamoorthy and M. Ravichandran, “Synthesis of metal matrix composites via powder metallurgy route: a review,” *Mechanics and Mechanical Engineering*, vol. 22, no. 1, pp. 65–76, 2018.
- [13] R. Narayanasamy, T. Ramesh, and K. S. Pandey, “Workability studies on cold upsetting of Al- Al<sub>2</sub>O<sub>3</sub> composite material,” *Materials & Design*, vol. 27, no. 7, pp. 566–575, 2006.
- [14] M. Delavari, A. Salarvand, A. Rahi, and F. Shahri, “The effect of powder metallurgy process parameters on mechanical properties of micro and nano-iron powder,” *International Journal of Engineering, Science and Technology*, vol. 3, no. 9, pp. 86–94, 2011.
- [15] R. U. Din, Q. A. Shafqat, Z. G. H. ZahidAsghara et al., “Microstructural evolution, powder characteristics, compaction behavior and sinterability of Al 6061–B4C composites as a function of reinforcement content and milling times,” *Russian Journal of Non-Ferrous Metals*, vol. 59, no. 2, pp. 207–222, 2018.
- [16] N. Showaiter and M. Youseffi, “Compaction, sintering and mechanical properties of elemental 6061 Al powder with and without sintering aids,” *Materials & Design*, vol. 29, no. 4, pp. 752–762, 2008.
- [17] O. Joo Won, S. K. Ryu, W. S. Lee, and S. J. Park, “Analysis of compaction and sintering behavior of 316L stainless steel nano/micro bimodal powder,” *Powder Technology*, vol. 322, pp. 1–8, 2017.
- [18] V. V. Vani and S. K. Chak, “The effect of process parameters in aluminum metal matrix composites with powder metallurgy,” *Manufacturing Review*, vol. 5, pp. 1–13, 2018.
- [19] M. D. Zakir Hussain, S. Khan, and P. Sarmah, “Optimization of powder metallurgy processing parameters of Al<sub>2</sub>O<sub>3</sub>/Cu composite through Taguchi method with grey relational analysis,” *Journal of King Saud University - Engineering Sciences*, vol. 31, pp. 1–13, 2019.
- [20] T. Pravin, M. Sadhasivam, and S. Raghuraman, “Optimization of process parameters of Al-10% Cu compacts through powder metallurgy,” *Applied Mechanics and Materials*, vol. 813-814, pp. 603–607, 2010.
- [21] M. Ravichandran and V. Anandkrishnan, “Optimization of powder metallurgy parameters to attain maximum strength coefficient in Al-10 wt% MoO<sub>3</sub>composite,” *Journal of Materials Research*, vol. 30, no. 15, pp. 2380–2387, 2015.
- [22] M. Ravichandran, A. Naveen Sait, and V. Anandkrishnan, “Workability studies on Al+2.5%TiO<sub>2</sub>+Gr powder metallurgy composites during cold upsetting,” *Materials Research*, vol. 17, no. 6, pp. 1–13, 2014.
- [23] H. T. Son, T. S. Kim, C. Suryanarayana, and B. S. Chun, “Homogeneous dispersion of graphite in a 6061 aluminum alloy by ball milling,” *Materials Science and Engineering A*, vol. 348, no. 1-2, pp. 163–169, 2003.
- [24] D. Jeyasimman, S. Sivasankaran, K. Sivaprasad, R. Narayanasamy, and R. S. Kambali, “An investigation of the synthesis, consolidation and mechanical behaviour of Al 6061 nanocomposites reinforced by TiC via mechanical alloying,” *Materials & Design*, vol. 57, pp. 394–404, 2014.
- [25] S. J. Hong and P. W. Kao, “SiC-reinforced aluminium composite made by resistance sintering of mechanically alloyed powders,” *Materials Science and Engineering A*, vol. 119, pp. 153–159, 1989.
- [26] D. Srinivasan, M. Meignanamoorthy, and M. Ravichandran, “Optimization of process parameters of boron carbide filled aluminium matrix composites using grey Taguchi method,” *Materials Research Express*, vol. 6, no. 7, article 076504, 2019.
- [27] S. Marichamy, M. Saravanan, M. Ravichandran, and G. Veerappan, “Parametric optimization of electrical discharge machining process on  $\alpha$ - $\beta$  brass using grey relational analysis,” *Journal of Materials Research*, vol. 31, no. 16, pp. 2531–2537, 2016.
- [28] V. Umasankar, M. Anthony Xavier, and S. Karthikeyan, “Experimental evaluation of the influence of processing parameters on the mechanical properties of SiC particle reinforced AA6061 aluminium alloy matrix composite by powder processing,” *Journal of Alloys and Compounds*, vol. 582, pp. 380–386, 2014.
- [29] M. Dewidar, M. B. G. T. Abdel-Jaber, and H. Badry, “Effect of processing parameters and amount of additives on the mechanical properties and wear resistance of copper-based composite,” *International Journal of Mechanical & Mechatronics Engineering*, vol. 10, no. 3, pp. 20–26, 2010.
- [30] M. Rahimian, N. Ehsani, N. Parvin, and H. R. Baharvandi, “The effect of sintering temperature and the amount of reinforcement on the properties of Al-Al<sub>2</sub>O<sub>3</sub> composite,” *Materials & Design*, vol. 30, no. 8, pp. 3333–3337, 2009.
- [31] Z. Hussain and L. C. Kit, “Properties and spot welding behaviour of copper-alumina composites through ball milling and mechanical alloying,” *Materials & Design*, vol. 29, no. 7, pp. 1311–1315, 2008.
- [32] G. K. Meenashisundaram, S. Seetharaman, and M. Gupta, “Enhancing overall tensile and compressive response of pure Mg using nano- TiB<sub>2</sub> particulates,” *Materials Characterization*, vol. 94, pp. 178–188, 2014.
- [33] O. El-Kady and A. Fathy, “Effect of SiC particle size on the physical and mechanical properties of extruded Al matrix nanocomposites,” *Materials & Design*, vol. 54, pp. 348–353, 2014.
- [34] C. Li, R. Qiu, B. Luan, and Z. Li, “Effect of carbon nanotubes and high temperature extrusion on the microstructure evolution of Al-Cu alloy,” *Materials Science and Engineering A*, vol. 704, pp. 38–44, 2017.
- [35] C.-A. Wang and L. F. Hu, “Effect of sintering temperature on compressive strength of porous yttria-stabilized zirconia composites,” *Ceramics International*, vol. 36, no. 5, pp. 1697–1701, 2010.
- [36] A. Wagih, A. Fathy, and T. A. Sebaey, “Experimental investigation on the compressibility of Al/Al<sub>2</sub>O<sub>3</sub> nanocomposites,” *International Journal of Materials and Product Technology*, vol. 52, no. 3/4, pp. 312–332, 2016.
- [37] M. Rahimian, N. Ehsani, N. Parvin, H. r. Baharvandi, and H. R. Baharvandi, “The effect of particle size, sintering temperature and sintering time on the properties of Al-Al<sub>2</sub>O<sub>3</sub> composites, made by powder metallurgy,” *Journal of Materials Processing Technology*, vol. 209, no. 14, pp. 5387–5393, 2009.

- [38] P. Balamurugan and M. Uthayakumar, "Influence of process parameters on Cu-Fly ash composite by powder metallurgy technique," *Materials and Manufacturing Processes*, vol. 30, no. 3, pp. 313–319, 2015.
- [39] C. C. Tsao, "Grey-Taguchi method to optimize the milling parameters of aluminum alloy," *International Journal of Advanced Manufacturing Technology*, vol. 40, no. 1-2, pp. 41–48, 2009.
- [40] H. Siddhi Jailani, A. Rajadurai, B. Mohan, A. Senthil Kumar, and T. Sornakumar, "Multi-response optimisation of sintering parameters of Al-Si alloy/fly ash composite using Taguchi method and grey relational analysis," *The International Journal of Advanced Manufacturing Technology*, vol. 45, no. 3-4, pp. 362–369, 2009.
- [41] N. Tosun, "Determination of optimum parameters for multi-performance characteristics in drilling by using grey relational analysis," *The International Journal of Advanced Manufacturing Technology*, vol. 28, no. 5-6, pp. 450–455, 2006.
- [42] M. K. Ho, K. S. Pil, K. Dae-Gun, and K. Y. Do, "Sintering characteristic of Al<sub>2</sub>O<sub>3</sub>-reinforced 2xxx series Al composite powders," *Journal of Alloys and Compounds*, vol. 400, no. 1-2, pp. 150–153, 2005.